C. R. Mecanique 346 (2018) 48–56

Contents lists available at ScienceDirect

Comptes Rendus Mecanique

www.sciencedirect.com

Microscopic modelling of orientation kinematics of non-spherical particles suspended in confined flows using unilateral mechanics

Adrien Scheuer [a,b], Emmanuelle Abisset-Chavanne [a], Francisco Chinesta [c,*], Roland Keunings [b]

[a] ICI – Institut de calcul intensif & ESI GROUP Chair, École centrale de Nantes, 1, rue de la Noe, 44300 Nantes, France
[b] ICTEAM, Université catholique de Louvain, avenue Georges-Lemaître 4, B-1348 Louvain-la-Neuve, Belgium
[c] PIMM & ESI GROUP Chair, ENSAM ParisTech, 151, boulevard de l'Hôpital, 75013 Paris, France

ARTICLE INFO

Article history:
Received 5 July 2017
Accepted 8 November 2017
Available online 1 December 2017

Keywords:
Fibre suspensions
Jeffery's equation
Confinement

ABSTRACT

The properties of reinforced polymers strongly depend on the microstructural state, that is, the orientation state of the fibres suspended in the polymeric matrix, induced by the forming process. Understanding flow-induced anisotropy is thus a key element to optimize both materials and process. Despite the important progresses accomplished in the modelling and simulation of suspensions, few works addressed the fact that usual processing flows evolve in confined configurations, where particles characteristic lengths may be greater than the thickness of the narrow gaps in which the flow takes place. In those circumstances, orientation kinematics models proposed for unconfined flows must be extended to the confined case. In this short communication, we propose an alternative modelling framework based on the use of unilateral mechanics, consequently exhibiting a clear analogy with plasticity and contact mechanics. This framework allows us to revisit the motion of confined particles in Newtonian and non-Newtonian matrices. We also prove that the confined kinematics provided by this model are identical to those derived from microstructural approaches (Perez et al. (2016) [1]).

1. Introduction

Over the last decades, composite materials, made of a suspending matrix and a reinforcement composed of fibres used to fortify the matrix in terms of strength and stiffness, were successfully introduced in the aerospace and automotive industries and proved to be a lightweight alternative to produce structural and functional parts. The mechanical properties of such reinforced polymers, however, strongly depend on the orientation state of their microstructure, which is established during the forming process [2]. Predicting the evolution of this orientation state is thus a key yet complex task, since the motion of the reinforcing fibres is impacted by the flowing matrix and the interactions with the neighbouring fibres and cavity walls. Thus, flow-induced anisotropy must be understood and modelled in order to optimize both materials and processes.

* Corresponding author.
E-mail addresses: Adrien.Scheuer@ec-nantes.fr, Adrien.Scheuer@uclouvain.be (A. Scheuer), Emmanuelle.Abisset-chavanne@ec-nantes.fr (E. Abisset-Chavanne), Francisco.Chinesta@ensam.edu (F. Chinesta), Roland.Keunings@uclouvain.be (R. Keunings).

https://doi.org/10.1016/j.crme.2017.11.003

There is a long history of studies of the motion of slender bodies suspended in a viscous fluid, starting from the seminal work of Jeffery back in 1922 [3]. A vast literature dedicated to fibre and non-spherical particle suspensions is available, studying extensively different modelling scales and exploring the impact of the concentration regime and the nature of the suspending matrix. Schematically, the three main modelling scales involved when addressing the orientation kinematics of suspended particles can be summarized as follows: (i) the *microscopic* scale, the scale of a single particle; (ii) the *mesoscopic* scale, the scale of a population of particle, whose conformation is usually represented by a probability density function (pdf) of orientation, giving an unambiguous and complete description of the orientation state; and (iii) the *macroscopic* scale, the scale of the part, whose conformation is often given by the first moments of the aforementioned pdf, providing a coarse yet concise description of the orientation state in the part. Depending on the level of detail and accuracy required for a given application, a specific scale, or a combination of them might be chosen. For further detail on that subject, including the so-called multiscale approach, we refer the reader to the review [4] and the monograph [5], as well as to the references therein. Only a succinct overview of the microscopic modelling is proposed thereafter.

In [3], Jeffery derived the expression of the hydrodynamic torque exerted on an ellipsoidal particle immersed in an unbounded creeping flow of a Newtonian fluid. He then obtained an equation of motion by assuming that the particle rotates so as to achieve instantaneous zero torque, resulting in the so-called Jeffery equation. Considering a spheroid (axisymetric ellipsoid) and defining the orientation of a particle by the unit vector $\mathbf{p}$ along its principal axis, Jeffery's equation reads

$$\dot{\mathbf{p}}^J = \boldsymbol{\Omega}\cdot\mathbf{p} + \kappa(\mathbf{D}\cdot\mathbf{p} - (\mathbf{D}:(\mathbf{p}\otimes\mathbf{p})\mathbf{p})) \tag{1}$$

where $\boldsymbol{\Omega}$ and $\mathbf{D}$ are, respectively, the skew-symmetric and symmetric parts of the unperturbed velocity gradient $\nabla\mathbf{v}$ of the flow, and κ is the shape factor of the spheroid, given by $\kappa = \frac{r^2-1}{r^2+1}$ with r the aspect ratio of the particle. Slender bodies like fibres and rods can be assimilated as infinite aspect ratio ellipsoids ($\kappa \approx 1$).

Jeffery's equation was experimentally verified by Taylor [6] and Mason [7]. Bretherton [8] showed that the equation is also valid for any axisymmetric particle provided that an effective aspect ratio is determined. Hinch and Leal [9–12] also studied Jeffery's model, addressing the impact of Brownian motion and proposing constitutive equations for the behaviour of suspensions. However, only a few works, either experimental [13,14] or numerical and theoretical [15,16], address the fact that flows of industrial interest take place in narrow gaps, whose thickness is of the same order of magnitude or smaller than the length of the reinforcing fibres, thus constraining the space of possible orientation, and as a consequence the kinematics.

In [1], we proposed a multiscale model to describe the orientation development of a dilute suspension of fibres confined in a narrow gap. The microscopic model was based on a dumbbell representation [17] of the confined rod, with hydrodynamic and contact forces (normal to the gap wall) acting on it. This confinement model was later extended in [18] to include unilateral contacts and non-uniform strain rates at the scale of the rod. In any case, the resulting kinematics are a combination of the unconfined Jeffery kinematics and a correction term that prevents the fibre from leaving the flow domain, that is,

$$\dot{\mathbf{p}} = \dot{\mathbf{p}}^J + \dot{\mathbf{p}}^C \tag{2}$$

The equation of motion of such a confined rod, derived in [1] and summarized in Eq. (2), presents thus significant similarities with equations of elastoplaticity. Indeed, we could draw a parallel between, on the one hand, the classical unconfined kinematics and the elastic deformation, and, on the other hand, the confined motion of the particle and elastoplatic deformation.

Hence, the purpose of this short communication is to explore the alternative modelling framework based on unilateral mechanics to revisit the motion of confined particles in Newtonian and non-Newtonian matrices.

The paper is organised as follows. In Section 2, we derive the model for the confined kinematics of suspended particles using unilateral mechanics. Then, in Section 3, we discuss how this general framework allows us to build the confined kinematics of fibres and spheroids immersed in a Newtonian (based on Jeffery's model [3]) or second-order (based on Brunn's model [19]) viscoelastic fluid. Finally, in Section 4, we draw the main conclusions and present some perspectives of this approach.

Remark. In this paper, we consider the following tensor products, assuming Einstein's summation convention:

- if $\mathbf{a}$ and $\mathbf{b}$ are first-order tensors, then the single contraction "$\cdot$" reads $(\mathbf{a}\cdot\mathbf{b}) = a_j\ b_j$;
- if $\mathbf{a}$ and $\mathbf{b}$ are first-order tensors, then the dyadic product "$\otimes$" reads $(\mathbf{a}\otimes\mathbf{b})_{jk} = a_j\ b_k$;
- if $\mathbf{a}$ and $\mathbf{b}$ are respectively second and first-order tensors, then the single contraction "$\cdot$" reads $(\mathbf{a}\cdot\mathbf{b})_j = a_{jk}\ b_k$;
- if $\mathbf{a}$ and $\mathbf{b}$ are second-order tensors, then the double contraction ":" reads $(\mathbf{a}:\mathbf{b}) = a_{jk}\ b_{kj}$.

2. Confined orientation kinematics using unilateral mechanics

In this section, we derive step by step the kinematics of a confined suspended particle using the framework of unilateral mechanics.

(i) *Additive decomposition.* We assume that the particle kinematics (particle rotary velocity) can be decomposed into an unconfined (U) and confined (C) contribution, according to

$$\dot{\mathbf{p}} = \dot{\mathbf{p}}^{\mathrm{U}} + \dot{\mathbf{p}}^{\mathrm{C}} \tag{3}$$

By definition, the orientation vector is subject to the normalization condition

$$\mathbf{p} \cdot \mathbf{p} = 1 \tag{4}$$

(ii) *Unconfined contribution.* The unconfined equation of motion $\dot{\mathbf{p}}^{\mathrm{U}}$ is either given by a model from the literature, e.g., Jeffery's equation [3] for ellipsoidal particles immersed in a Newtonian fluid or Brunn's model [19] in the case of a second-order (non-Newtonian) matrix, or could be estimated from experimental observations. In order to satisfy the normalization condition Eq. (4), the unconfined kinematics should verify $\dot{\mathbf{p}}^{\mathrm{U}} \cdot \mathbf{p} = 0$.

(iii) *Allowed domain and confinement condition.* We define a function $f : \mathcal{S} \to \mathbb{R}$ called the confinement condition (the equivalent of the yield condition in plasticity mechanics) and constrain the admissible orientation states $\mathbf{p} \in \mathcal{S}$ (with $\mathcal{S}$ the unit sphere) to lie in the flow domain $\mathcal{D}$, ensuring the gap walls' impenetrability, defined as

$$\mathcal{D} = \left\{ \mathbf{p} \in \mathcal{S} \mid f(\mathbf{p}) = \mathbf{p} \cdot \mathbf{n} - \frac{H}{L} \leq 0 \right\} \tag{5}$$

where L is the semi-length of the particle, H the gap semi-width, and $\mathbf{n}$ denotes a unit vector normal to the gap wall. We assume, without loss of generality, that $\mathbf{p}$ points towards the upper hemisphere.
We refer to the interior of $\mathcal{D}$, denoted by $\mathrm{int}(\mathcal{D})$ and defined as $\mathrm{int}\mathcal{D}) = \{\mathbf{p} \in \mathcal{S} \mid f(\mathbf{p}) < 0\}$, as the unconfined domain, whereas the boundary $\partial\mathcal{D}$, given by $\partial\mathcal{D} = \{\mathbf{p} \in \mathcal{S} \mid f(\mathbf{p}) = 0\}$, is called the confinement surface.

(iv) *Confined contribution and consistency requirement.* The confined kinematics $\dot{\mathbf{p}}^{\mathrm{C}}$ is obtained from the gradient of the confinement condition introduced above, *i.e.*

$$\dot{\mathbf{p}}^{\mathrm{C}} = -\gamma \frac{\mathrm{d}f}{\mathrm{d}\mathbf{p}} \tag{6}$$

where γ is the consistency parameter. The derivative of $f(\mathbf{p})$ with respect to $\mathbf{p}$, enforcing the normalization condition, reads

$$\frac{\mathrm{d}f}{\mathrm{d}\mathbf{p}} = \mathbf{n} - (\mathbf{p} \cdot \mathbf{n})\mathbf{p} \tag{7}$$

which is obtained by subtracting from the derivative of $f(\mathbf{p})$ with respect to $\mathbf{p}$ its projection onto the $\mathbf{p}$ direction in order to ensure that $\dot{\mathbf{p}}^{\mathrm{C}} \cdot \mathbf{p} = 0$.
The consistency parameter γ is assumed, on the one hand, to obey the Kuhn–Tucker complementary conditions

$$\gamma \geq 0, \qquad f(\mathbf{p}) \leq 0, \qquad \text{and} \qquad \gamma f(\mathbf{p}) = 0 \tag{8}$$

and, on the other hand, to satisfy the consistency requirement

$$\gamma \dot{f}(\mathbf{p}) = 0 \tag{9}$$

To obtain the derivative of f with respect to time, we proceed as follows:

$$\dot{f} = \frac{\mathrm{d}f}{\mathrm{d}\mathbf{p}} \cdot \dot{\mathbf{p}} \tag{10}$$

$$= (\mathbf{n} - (\mathbf{p} \cdot \mathbf{n})\mathbf{p}) \cdot (\dot{\mathbf{p}}^{\mathrm{U}} - \gamma(\mathbf{n} - (\mathbf{p} \cdot \mathbf{n})\mathbf{p})) \tag{11}$$

$$= \dot{\mathbf{p}}^{\mathrm{U}} \cdot \mathbf{n} - \gamma(1 - (\mathbf{p} \cdot \mathbf{n})^2) \tag{12}$$

Thus the value of γ is given by

$$\gamma = \frac{(\dot{\mathbf{p}}^{\mathrm{U}} \cdot \mathbf{n})}{(1 - (\mathbf{p} \cdot \mathbf{n})^2)} \tag{13}$$

(v) *Summary.* The resulting kinematics can be summarized as follows:

$$\begin{aligned} & f < 0 \Longleftrightarrow \mathbf{p} \in \mathrm{int}(\mathcal{D}),\ \gamma = 0 \Longrightarrow \dot{\mathbf{p}} = \dot{\mathbf{p}}^{\mathrm{U}} && \text{unconfined} \\ & f = 0 \Longleftrightarrow \mathbf{p} \in \partial\mathcal{D}, \quad \begin{cases} \dot{f} = 0 \text{ and } \gamma > 0 \Longrightarrow \dot{\mathbf{p}} = \dot{\mathbf{p}}^{\mathrm{U}} + \dot{\mathbf{p}}^{\mathrm{C}} & \text{confinement} \\ \dot{f} = 0 \text{ and } \gamma = 0 \Longrightarrow \dot{\mathbf{p}} = \dot{\mathbf{p}}^{\mathrm{U}} & \text{force-free contact} \\ \dot{f} < 0 \Longrightarrow \gamma = 0 \Longrightarrow \dot{\mathbf{p}} = \dot{\mathbf{p}}^{\mathrm{U}} & \text{unconfined detachment} \end{cases} \end{aligned} \tag{14}$$

The force-free contact actually corresponds to the case where the confined particle is touching the gap wall, but is not trying to leave the flow domain (to "push" on the wall).

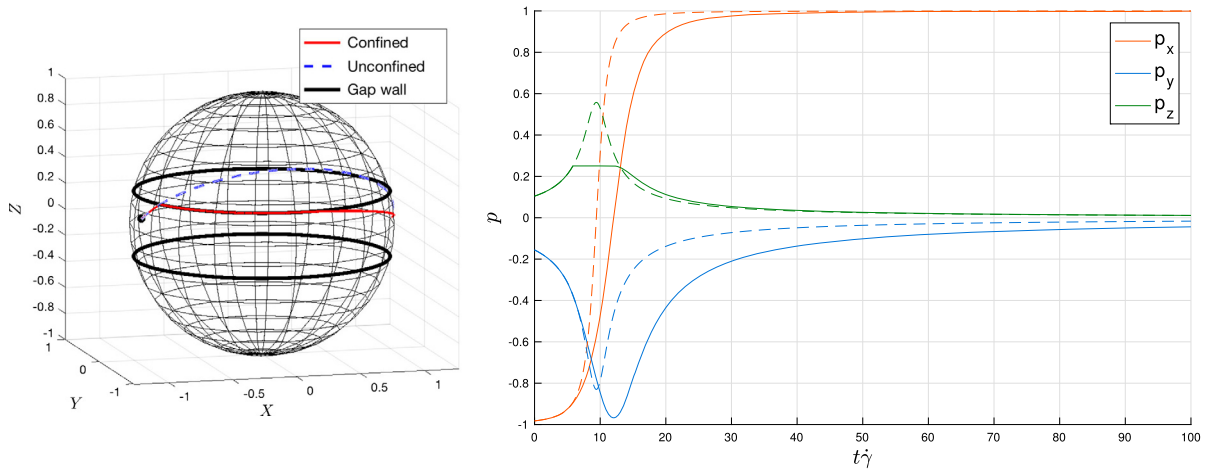

(a) Particle trajectory (b) Components of the orientation vector $\mathbf{p}$

Fig. 1. Confined rod suspended in a Newtonian fluid (solid line: confined particle; dotted line: unconfined particle).

Remark 2.1. For the sake of clarity, we assumed in the present section and throughout the remainder of this article that under confinement, both extremities of the suspended particle are in contact with the gap walls and the centre of gravity of the particle is fixed in the mid-plane of the flow channel. These assumptions are, however, relaxed in Appendix A, where we address, using the same framework just introduced, the general case by introducing the position of the particle centre of gravity in the confinement condition, allowing in the meantime contact with only one gap wall.

3. Discussion

The confined kinematics obtained in the previous section read

$$\dot{\mathbf{p}} = \dot{\mathbf{p}}^{\mathrm{U}} + \dot{\mathbf{p}}^{\mathrm{C}} = \dot{\mathbf{p}}^{\mathrm{U}} - \frac{(\dot{\mathbf{p}}^{\mathrm{U}} \cdot \mathbf{n})}{(1 - (\mathbf{p} \cdot \mathbf{n})^2)} (\mathbf{n} - (\mathbf{p} \cdot \mathbf{n})\mathbf{p}) \tag{15}$$

which coincides exactly with the expression obtained in [1] following a microstructural approach for a confined rod immersed in a Newtonian fluid ($\dot{\mathbf{p}}^{\mathrm{U}}$ was thus given by Jeffery's kinematics).

However, the unilateral mechanics approach developed in the previous section does not assume anything on the shape of the suspended particles or the nature of the matrix fluid. Only an expression of the unconfined kinematics is actually necessary, which allows us to extend straightforwardly our model describing the motion of a confined particle to situations where the microstructural approach from [1] might be tedious.

In this section, we thus discuss three scenarios: (i) a rod immersed in a Newtonian fluid (developed in [1]), (ii) a spheroid in a Newtonian fluid, and (iii) a spheroid in a second-order fluid. We also provide some numerical illustrations in the case of a linear shear flow $\mathbf{v} = \begin{bmatrix} \dot{\gamma} z & 0 & 0 \end{bmatrix}^{\mathrm{T}}$, with $\dot{\gamma} = 1$ in a channel of height $H = 0.25\,L$

3.1. Confined rod suspended in a Newtonian fluid

Inserting Jeffery's equation for rods $\dot{\mathbf{p}}^{\mathrm{J}}_{\mathrm{rod}} = \nabla\mathbf{v} \cdot \mathbf{p} - (\nabla\mathbf{v} : (\mathbf{p} \otimes \mathbf{p})\mathbf{p})$ as unconfined kinematics in Eq. (15), we recover the kinematics derived in [1] using a microstructural approach (hydrodynamic and contact forces acting on the dumbbell representation of a rod).

Fig. 1 depicts the evolution of the orientation of a rigid fibre immersed in a shear flow of a Newtonian fluid. The solid line shows the trajectory of the confined rod and the dotted line the trajectory of an hypothetical unconfined particle starting from the same initial orientation. Fig. 1a shows the evolution of the rod orientation as a trajectory on the unit sphere. Starting from the same initial condition, the confined (solid red) and unconfined (dotted blue) rods both follow the same Jeffery orbit. When it touches the wall, the confined rod is constrained to slide along the gap wall, and finally catches an unconfined Jeffery orbit tangent to the wall and aligns in the flow. This abrupt change in the trajectory as it touches the gap wall can also be observed in Fig. 1b, where the components of the unit vector of orientation $\mathbf{p}$ are represented.

3.2. Confined ellipsoid suspended in a Newtonian fluid

Considering spheroidal particles (axisymmetric ellipsoids), we insert now the general Jeffery equation [Eq. (1)] in Eq. (15). The equivalence with the kinematics obtained from a microstructural approach on a tri-dumbbell is detailed in Appendix B.

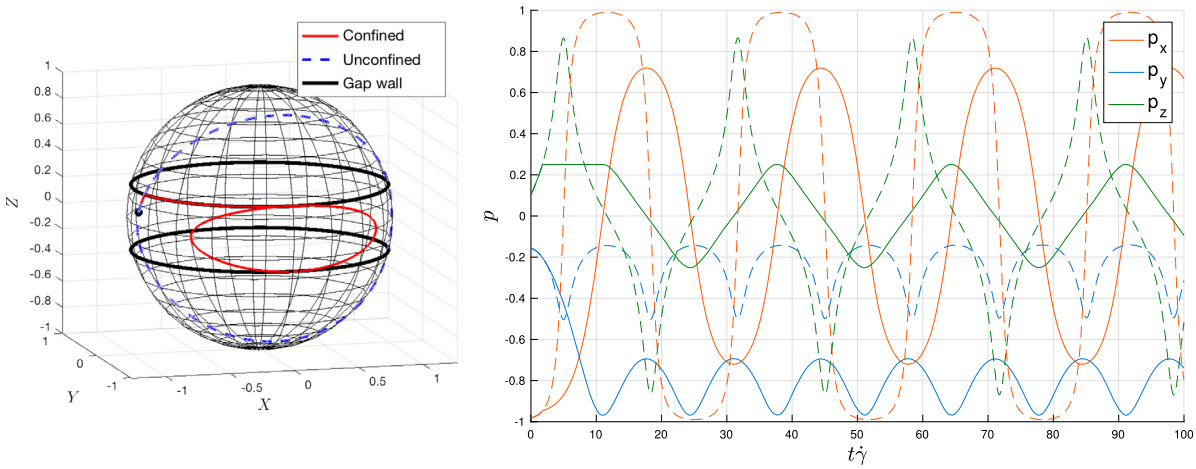

(a) Particle trajectory (b) Components of the orientation vector $\mathbf{p}$

Fig. 2. Confined spheroid (aspect ratio $r = 4$) suspended in a Newtonian fluid (solid line: confined particle; dotted line: unconfined particle).

Fig. 2 depicts the evolution of the orientation of a spheroid of aspect ratio $r = 4$ immersed in the same shear flow of a Newtonian fluid. The unconfined particle (dotted blue) undergoes its classical kayaking motion, whereas the confined one (solid red) first slides along the wall, and is then constrained on the largest kayaking orbit possible in the narrow gap, that is, the orbit tangent to both gap walls. Note that the orbit points tangent to the channel walls thus correspond to force-free contacts.

3.3. Confined ellipsoid suspended in a second-order fluid

Leal [20] and Brunn [19] published some important theoretical works to describe, respectively, the motion of a rod and an ellipsoid in a second-order fluid, in the limit of low Weissenberg numbers, which constitutes the counterpart of Jeffery's equation in the case of a viscoelastic suspending matrix. The constitutive equation for the second-order fluid is given by Giesekus [21]

$$\boldsymbol{\sigma} = -p\mathbf{I} + 2\eta\mathbf{D} + 2\eta\left[k_0^{(11)}\mathbf{D}\cdot\mathbf{D} + k_0^{(2)}\left(\frac{\partial\mathbf{D}}{\partial t} + \mathbf{v}\cdot\nabla\mathbf{D} + \boldsymbol{\Omega}\cdot\mathbf{D} - \mathbf{D}\cdot\boldsymbol{\Omega}\right)\right] \tag{16}$$

where $k_0^{(11)}$ and $k_0^{(2)}$ are material parameters. Brunn [19] derived the equation of evolution of the orientation of a particle, and the resulting kinematics reads

$$\dot{\mathbf{p}}^B = \boldsymbol{\Omega}\cdot\mathbf{p} + \kappa(\mathbf{D}\cdot\mathbf{p} - (\mathbf{D}:(\mathbf{p}\otimes\mathbf{p})\mathbf{p})) - (\mathbf{I} - \mathbf{p}\otimes\mathbf{p})\cdot\mathbf{D}\cdot(H_2\mathbf{D}\cdot\mathbf{p} + H_1(\mathbf{D}:(\mathbf{p}\otimes\mathbf{p}))\mathbf{p}) \tag{17}$$

where H_1 and H_2 depend on the material parameters and the ellipsoid aspect ratio as given in Brunn [19].

In Appendix C, we briefly show how to write Brunn's kinematics [Eq. (17)] in the form of Jeffery's kinematics Eq. (1) with an effective velocity gradient $\tilde{\nabla}\mathbf{v}$. Consequently, the microstructural validation developed in Appendix B can also be used in this section.

In the case of a second-order fluid, it is well known that the kayaking motion of the particle drifts towards the shear plane for oblate spheroids ($r < 1$) or towards the vorticity axis for prolate spheroids ($r > 1$) [19,22,23].

Fig. 3 depicts the evolution of the orientation of a spheroid of aspect ratio $r = 4$ immersed in the same shear flow, but now the suspending matrix is a second-order fluid (in this illustration, we have $k_0^{(11)} = 0.144$ and $k_0^{(11)} = -0.09$, and thus, $H_1 = 0.084$ and $H_2 = 0.0056$). Again, the confined spheroid (solid red) is constrained to exert its kayaking and drifting motion towards the vorticity axis of the flow in the narrow flow domain.

4. Conclusion and perspectives

This work proposes an alternative route for deriving the confined orientation kinematics of dilute suspensions of fibres and ellipsoidal particles. This approach, based on unilateral mechanics, allows us to extend directly our previous microstructural model developed for confined rods in a Newtonian fluid [1] to ellipsoidal particles and viscoelastic matrices.

The same strategy might then be applied at the macroscopic scale, working on the so-called second-order orientation tensor $\mathbf{a}$ [24], $\mathbf{a} = \int(\mathbf{p}\otimes\mathbf{p})\ \psi(\mathbf{p})\ \mathrm{d}\mathbf{p}$, to derive a macroscopic model for confined suspensions. However, defining the adequate confinement condition $f(\mathbf{a}) \leq 0$ in that case is a delicate task that will be addressed in a future work.

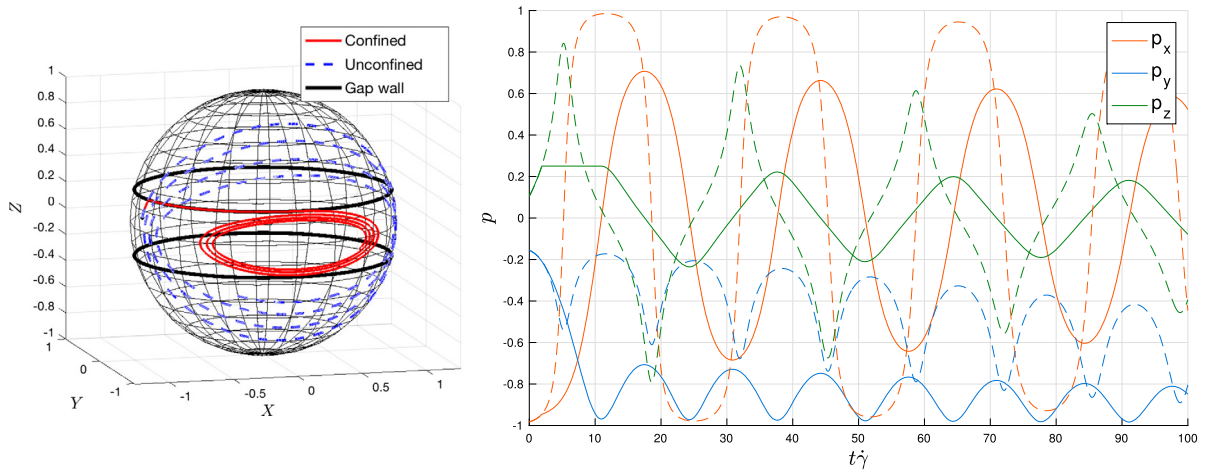

(a) Particle trajectory (b) Components of the orientation vector $\mathbf{p}$

Fig. 3. Confined spheroid (aspect ratio $r = 4$) suspended in a second-order fluid (solid line: confined particle – dotted line: unconfined particle).

Acknowledgements

A. Scheuer is a Research Fellow of the "Fonds de la recherche scientifique de Belgique" – F.R.S.–FNRS.

Appendix A. Confined orientation kinematics using unilateral mechanics – interaction with only one gap wall

In this appendix, we extend the framework introduced in Section 2 in situations where the suspended particle's centre of gravity does not necessarily lies in the channel mid-plane, allowing interaction with only one gap wall. In that case, the confinement condition now reads

$$f(\mathbf{p}) = (\mathbf{x}_G + \mathbf{p}L) \cdot \mathbf{n} \leq H \tag{18}$$

with $\mathbf{x}_G$ the position of the particle centre of gravity G. The allowed domain $\mathcal{D}$ is thus now given by

$$\mathcal{D} = \left\{ \mathbf{p} \in \mathcal{S} \mid f(\mathbf{p}) = \frac{1}{L}(\mathbf{x}_G \cdot \mathbf{n}) + (\mathbf{p} \cdot \mathbf{n}) - \frac{H}{L} \leq 0 \right\} \tag{19}$$

Note that in this case, we consider the case where G lies in the upper-half of the channel.

Using these new definitions, the derivation of the confined kinematics is obtained following the same rationale as that presented in the step (iv) in Section 2. The derivation of f with respect to $\mathbf{p}$ [Eq. (7)] is left unchanged, whereas the derivation of f with respect to time [Eq. (10)] now reads

$$\dot{f} = \frac{\partial f}{\partial \mathbf{x}_G} \cdot \dot{\mathbf{x}}_G + \frac{\partial f}{\partial \mathbf{p}} \cdot \dot{\mathbf{p}} \tag{20}$$

$$= \frac{1}{L}(\mathbf{n} \cdot \dot{\mathbf{x}}_G) + (\mathbf{n} - (\mathbf{p} \cdot \mathbf{n})\mathbf{p}) \cdot \dot{\mathbf{p}} \tag{21}$$

$$= \frac{1}{L}(\mathbf{n} \cdot \dot{\mathbf{x}}_G) + (\mathbf{n} - (\mathbf{p} \cdot \mathbf{n})\mathbf{p}) \cdot (\dot{\mathbf{p}}^U - \gamma(\mathbf{n} - (\mathbf{p} \cdot \mathbf{n})\mathbf{p})) \tag{22}$$

$$= \frac{1}{L}(\mathbf{v}_G \cdot \mathbf{n}) + (\dot{\mathbf{p}}^U \cdot \mathbf{n}) - \gamma(1 - (\mathbf{p} \cdot \mathbf{n})^2) \tag{23}$$

with $\mathbf{v}_G = \dot{\mathbf{x}}_G$ the velocity of the particle's centre of gravity. Finally, the value of the consistency parameter γ is given by

$$\gamma = \frac{\frac{1}{L}(\mathbf{v}_G \cdot \mathbf{n}) + (\dot{\mathbf{p}}^U \cdot \mathbf{n})}{(1 - (\mathbf{p} \cdot \mathbf{n})^2)} \tag{24}$$

leading to the following expression for the confined kinematics

$$\dot{\mathbf{p}} = \dot{\mathbf{p}}^U + \dot{\mathbf{p}}^C = \dot{\mathbf{p}}^U - \frac{\frac{1}{L}(\mathbf{v}_G \cdot \mathbf{n}) + (\dot{\mathbf{p}}^U \cdot \mathbf{n})}{(1 - (\mathbf{p} \cdot \mathbf{n})^2)}(\mathbf{n} - (\mathbf{p} \cdot \mathbf{n})\mathbf{p}) \tag{25}$$

This expression is exactly the one that we derived in [18] when addressing the kinematics of a confined particle interacting with only one gap wall using a microstructural approach (dumbbell).

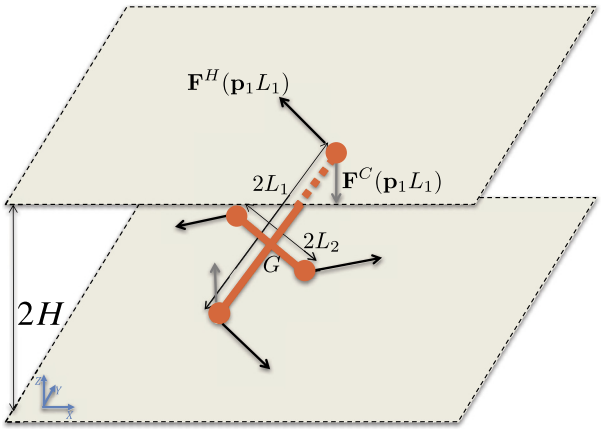

Fig. 4. Hydrodynamic and contact forces acting on a confined suspended spheroid.

Appendix B. Confined kinematics of an ellipsoid using the dumbbell approach

In order to address the confined kinematics of an ellipsoid immersed in a Newtonian fluid flow, we consider its corresponding tri-dumbbell representation. For the sake of simplicity, we consider in this appendix the 2D case, that is the bi-dumbbell represented in Fig. 4, which will provide the orientation kinematics of a spheroid (axisymmetric ellipsoid). The orientation of the two principle axes are given by the unit vectors $\mathbf{p}_1$ and $\mathbf{p}_2$.

On each bead acts a hydrodynamic force (Stokes drag), scaling with the difference of velocity between the fluid at the bead position and the bead itself. For the bead located at $\mathbf{p}_1 L_1$, that force reads

$$\mathbf{F}^{\mathrm{H}}(\mathbf{p}_1 L_1) = \xi(\mathbf{v}_0 + \nabla\mathbf{v}\cdot\mathbf{p}_1 L_1 - \mathbf{v}_{\mathrm{G}} - \dot{\mathbf{p}}_1 L_1) \tag{26}$$

where ξ is a friction coefficient and $\mathbf{v}_{\mathrm{G}}$ and $\mathbf{v}_0$ denote respectively the velocity of the centre of gravity G and the velocity of the fluid at G. Without any loss of generality, we assume that L_1 is the spheroid longest axis, on which contact with the gap wall will occur. The contact forces on the upper and lower beads read

$$\mathbf{F}^{\mathrm{C}}(\mathbf{p}_1 L_1) = \mu\mathbf{n} \qquad \text{and} \qquad \mathbf{F}^{\mathrm{C}}(-\mathbf{p}_1 L_1) = -\mu\mathbf{n} \tag{27}$$

with $\mathbf{n} = \begin{bmatrix} 0 & 0 & 1 \end{bmatrix}^{\mathrm{T}}$ (since the contact force is orthogonal to the wall as soon as friction is neglected – it could be easily introduced), and its intensity μ is a priori unknown.

When both beads of the dumbbell aligned along direction $\mathbf{p}_1$ are in contact with the gap walls (more general situations were analysed in [18]), balance of forces yields

$$2\xi(\mathbf{v}_0 - \mathbf{v}_{\mathrm{G}}) = 0 \tag{28}$$

that is, $\mathbf{v}_0 = \mathbf{v}_{\mathrm{G}}$, the particle's centre of gravity is moving with the fluid velocity at that position.

Balance of torques thus yields

$$2\mathbf{p}_1 L_1 \times \left(\nabla\mathbf{v}\cdot\mathbf{p}_1 L_1 - \dot{\mathbf{p}}_1 L_1 + \frac{\mu}{\xi}\mathbf{n}\right) + 2\mathbf{p}_2 L_2 \times (\nabla\mathbf{v}\cdot\mathbf{p}_2 L_2 - \dot{\mathbf{p}}_2 L_2) = \mathbf{0} \tag{29}$$

Introducing the fact that $\dot{\mathbf{p}}_i = \boldsymbol{\omega}\times\mathbf{p}_i$, $i = 1, 2$ (with $\boldsymbol{\omega}$ the angular velocity vector), and taking into account that $\mathbf{p}_i \times \boldsymbol{\omega}\times\mathbf{p}_i = \boldsymbol{\omega}$, $i = 1, 2$, we have

$$\boldsymbol{\omega} = \frac{L_1}{L_1^2 + L_2^2}(\mathbf{p}_1 \times (\nabla\mathbf{v}\cdot\mathbf{p}_1 L_1 + \frac{\mu}{\xi}\mathbf{n})) + \frac{L_2}{L_1^2 + L_2^2}(\mathbf{p}_2 \times (\nabla\mathbf{v}\cdot\mathbf{p}_2 L_2)) \tag{30}$$

Thus, the spheroid rotary velocity is given by

$$\dot{\mathbf{p}}_1 = \boldsymbol{\omega}\times\mathbf{p}_1 = \frac{L_1}{L_1^2 + L_2^2}((\mathbf{p}_1 \times (\nabla\mathbf{v}\cdot\mathbf{p}_1 L_1 + \frac{\mu}{\xi}\mathbf{n}))\times\mathbf{p}_1) + \frac{L_2}{L_1^2 + L_2^2}((\mathbf{p}_2 \times (\nabla\mathbf{v}\cdot\mathbf{p}_2 L_2))\times\mathbf{p}_1) \tag{31}$$

Applying the triple vector product formula $(\mathbf{a}\times\mathbf{b})\times\mathbf{c} = (\mathbf{a}\cdot\mathbf{c})\mathbf{b} - (\mathbf{b}\cdot\mathbf{c})\mathbf{a}$, the previous equation reads:

$$\begin{aligned}\dot{\mathbf{p}}_1 = {} & \frac{L_1}{L_1^2 + L_2^2}((\nabla\mathbf{v}\cdot\mathbf{p}_1 L_1 + \frac{\mu}{\xi}\mathbf{n}) - ((\nabla\mathbf{v}\cdot\mathbf{p}_1 L_1)\cdot\mathbf{p}_1 + \frac{\mu}{\xi}(\mathbf{n}\cdot\mathbf{p}_1))\mathbf{p}_1) \\ & - \frac{L_2}{L_1^2 + L_2^2}(((\nabla\mathbf{v}\cdot\mathbf{p}_2 L_2)\cdot\mathbf{p}_1)\mathbf{p}_2)\end{aligned} \tag{32}$$

We now develop the last term of this equation in order to obtain an expression that only depends on $\mathbf{p}_1$. First, we decompose the velocity gradient according to $\nabla\mathbf{v} = \mathbf{D} + \boldsymbol{\Omega}$,

$$((\nabla\mathbf{v}\cdot\mathbf{p}_2)\cdot\mathbf{p}_1)\mathbf{p}_2 = ((\mathbf{D}\cdot\mathbf{p}_2)\cdot\mathbf{p}_1)\mathbf{p}_2 + ((\boldsymbol{\Omega}\cdot\mathbf{p}_2)\cdot\mathbf{p}_1)\mathbf{p}_2 \tag{33}$$

Then we develop each of these terms. Using the fact that $\mathbf{D}$ is symmetric, we have

$$((\mathbf{D}\cdot\mathbf{p}_2)\cdot\mathbf{p}_1)\mathbf{p}_2 = \mathbf{p}_2(\mathbf{p}_1^{\mathrm{T}}\cdot\mathbf{D}\cdot\mathbf{p}_2) = \mathbf{p}_2(\mathbf{p}_2^{\mathrm{T}}\cdot\mathbf{D}\cdot\mathbf{p}_1) = (\mathbf{p}_2\otimes\mathbf{p}_2)\cdot\mathbf{D}\cdot\mathbf{p}_1 \tag{34}$$

Since $\mathbf{p}_1$ and $\mathbf{p}_2$ are mutually perpendicular,

$$(\mathbf{p}_1\otimes\mathbf{p}_1) + (\mathbf{p}_2\otimes\mathbf{p}_2) = \mathbf{I} \tag{35}$$

and thus Eq. (34) now reads

$$((\mathbf{D}\cdot\mathbf{p}_2)\cdot\mathbf{p}_1)\mathbf{p}_2 = (\mathbf{I} - (\mathbf{p}_1\otimes\mathbf{p}_1))\cdot\mathbf{D}\cdot\mathbf{p}_1 \tag{36}$$

Similarly, using the fact that $\boldsymbol{\Omega}$ is skew-symmetric, we have

$$((\boldsymbol{\Omega}\cdot\mathbf{p}_2)\cdot\mathbf{p}_1)\mathbf{p}_2 = \mathbf{p}_2(\mathbf{p}_1^{\mathrm{T}}\cdot\boldsymbol{\Omega}\cdot\mathbf{p}_2) = -\mathbf{p}_2(\mathbf{p}_2^{\mathrm{T}}\cdot\boldsymbol{\Omega}\cdot\mathbf{p}_1) = -(\mathbf{p}_2\otimes\mathbf{p}_2)\cdot\boldsymbol{\Omega}\cdot\mathbf{p}_1 \tag{37}$$

and thus

$$((\boldsymbol{\Omega}\cdot\mathbf{p}_2)\cdot\mathbf{p}_1)\mathbf{p}_2 = -(\mathbf{I} - (\mathbf{p}_1\otimes\mathbf{p}_1))\cdot\boldsymbol{\Omega}\cdot\mathbf{p}_1 \tag{38}$$

Finally, coming back to Eq. (32), we have

$$\begin{aligned}\dot{\mathbf{p}}_1 = {} & \frac{L_1}{L_1^2+L_2^2}((\nabla\mathbf{v}\cdot\mathbf{p}_1 L_1 + \frac{\mu}{\xi}\mathbf{n}) - ((\nabla\mathbf{v}\cdot\mathbf{p}_1 L_1)\cdot\mathbf{p}_1 + \frac{\mu}{\xi}(\mathbf{n}\cdot\mathbf{p}_1))\mathbf{p}_1) \\ & - \frac{L_2^2}{L_1^2+L_2^2}(\mathbf{D}\cdot\mathbf{p}_1 - (\mathbf{p}_1\otimes\mathbf{p}_1)\cdot\mathbf{D}\cdot\mathbf{p}_1 - \boldsymbol{\Omega}\cdot\mathbf{p}_1 + (\mathbf{p}_1\otimes\mathbf{p}_1)\cdot\boldsymbol{\Omega}\cdot\mathbf{p}_1)\end{aligned} \tag{39}$$

or

$$\dot{\mathbf{p}}_1 = \boldsymbol{\Omega}\cdot\mathbf{p}_1 + \frac{L_1^2-L_2^2}{L_1^2+L_2^2}\mathbf{D}\cdot\mathbf{p}_1 - \frac{L_1^2-L_2^2}{L_1^2+L_2^2}(\mathbf{p}_1\otimes\mathbf{p}_1)\cdot\mathbf{D}\cdot\mathbf{p}_1 + \frac{L_1}{L_1^2+L_2^2}(\frac{\mu}{\xi}(\mathbf{n} - (\mathbf{n}\cdot\mathbf{p}_1)\mathbf{p}_1)) \tag{40}$$

The first part of Eq. (40) is actually the classical Jeffery equation for a spheroid, since $\frac{L_1^2-L_2^2}{L_1^2+L_2^2} = \frac{r^2-1}{r^2+1} = \kappa$ is the spheroid shape factor and the second part is thus the confinement contribution,

$$\dot{\mathbf{p}}_1 = \dot{\mathbf{p}}_1^{\mathrm{J}} + \frac{L_1}{L_1^2+L_2^2}(\frac{\mu}{\xi}(\mathbf{n} - (\mathbf{n}\cdot\mathbf{p}_1)\mathbf{p}_1)) \tag{41}$$

Imposing the impenetrability condition [1]

$$(\mathbf{v}_{\mathrm{G}} + \dot{\mathbf{p}}_1 L_1)\cdot\mathbf{n} = 0 \tag{42}$$

allows us to obtain the intensity μ of the contact force. Since the particle centre of gravity is in the mid-plane of the shear flow, $\mathbf{v}_{\mathrm{G}} = 0$ and thus

$$\dot{\mathbf{p}}_1 L_1\cdot\mathbf{n} = \dot{\mathbf{p}}_1{}^{\mathrm{J}} L_1\cdot\mathbf{n} + \frac{L_1^2}{L_1^2+L_2^2}(\frac{\mu}{\xi}(1 - (\mathbf{n}\cdot\mathbf{p}_1)^2)) = 0 \tag{43}$$

The value of μ is then given by

$$\mu = -\frac{L_1^2+L_2^2}{L_1^2}\frac{\xi L_1}{(1-(\mathbf{n}\cdot\mathbf{p}_1)^2)}(\dot{\mathbf{p}}_1{}^{\mathrm{J}}\cdot\mathbf{n}) \tag{44}$$

Eventually, the confined kinematics of a rigid spheroid are given, as expected, by

$$\dot{\mathbf{p}}_1 = \dot{\mathbf{p}}_1^{\mathrm{J}} - \frac{(\dot{\mathbf{p}}_1{}^{\mathrm{J}}\cdot\mathbf{n})}{(1-(\mathbf{n}\cdot\mathbf{p}_1)^2)}(\mathbf{n} - (\mathbf{n}\cdot\mathbf{p}_1)\mathbf{p}_1) \tag{45}$$

Appendix C. Rewriting Brunn's kinematics with an effective velocity gradient

Brunn's orientation kinematics for a spheroid particle immersed in a second-order fluid reads [19]:

$$\dot{\mathbf{p}}^{\mathrm{B}} = \boldsymbol{\Omega}\cdot\mathbf{p} + \kappa(\mathbf{D}\cdot\mathbf{p} - (\mathbf{D}:(\mathbf{p}\otimes\mathbf{p})\mathbf{p})) - (\mathbf{I}-\mathbf{p}\otimes\mathbf{p})\cdot\mathbf{D}\cdot(H_2\mathbf{D}\cdot\mathbf{p} + H_1(\mathbf{D}:(\mathbf{p}\otimes\mathbf{p}))\mathbf{p}) \tag{46}$$

where the spheroid shape factor is given by $\kappa = \frac{r^2-1}{r^2+1}$, with r the aspect-ratio of the particle, and H_1 and H_2 are given by Brunn, $H_1 = (r^2-1)H_2 = -2\left(\frac{r^2-1}{r^2+1}\right)^2\left(k_0^{(2)} + \frac{1}{4}k_0^{(11)}\right)$. Developing Eq. (46), we have

$$\begin{aligned}\dot{\mathbf{p}}^{\mathrm{B}} = {} & \boldsymbol{\Omega}\cdot\mathbf{p} + \kappa(\mathbf{D}\cdot\mathbf{p} - (\mathbf{D}:(\mathbf{p}\otimes\mathbf{p})\mathbf{p})) - H_2\mathbf{D}^2\cdot\mathbf{p} + H_2(\mathbf{p}\otimes\mathbf{p})\cdot\mathbf{D}^2\cdot\mathbf{p} \\ & - H_1(\mathbf{D}:(\mathbf{p}\otimes\mathbf{p}))\,\mathbf{D}\cdot\mathbf{p} + H_1(\mathbf{D}:(\mathbf{p}\otimes\mathbf{p}))\,(\mathbf{p}\otimes\mathbf{p})\cdot\mathbf{D}\cdot\mathbf{p}\end{aligned} \tag{47}$$

We now define an effective velocity gradient:

$$\tilde{\nabla}\mathbf{v} = \nabla\mathbf{v} - \frac{H_2}{\kappa}\mathbf{D}^2 - \frac{H_1}{\kappa}(\mathbf{D}:(\mathbf{p}\otimes\mathbf{p}))\mathbf{D} \tag{48}$$

and the effective vorticity and strain rate tensors $\tilde{\boldsymbol{\Omega}} = \frac{1}{2}\left(\tilde{\nabla}\mathbf{v} - \tilde{\nabla}\mathbf{v}^{\mathrm{T}}\right)$ and $\tilde{\mathbf{D}} = \frac{1}{2}\left(\tilde{\nabla}\mathbf{v} + \tilde{\nabla}\mathbf{v}^{\mathrm{T}}\right)$. Equipped with this effective velocity gradient, Brunn's kinematics Eq. (46) can be rewritten in the same form as Jeffery's kinematics [Eq. (1)], that is,

$$\dot{\mathbf{p}}^{\mathrm{B}} = \tilde{\boldsymbol{\Omega}}\cdot\mathbf{p} + \kappa(\tilde{\mathbf{D}}\cdot\mathbf{p} - (\tilde{\mathbf{D}}:(\mathbf{p}\otimes\mathbf{p})\mathbf{p})) \tag{49}$$

References

[1] M. Perez, A. Scheuer, E. Abisset-Chavanne, F. Chinesta, R. Keunings, A multi-scale description of orientation in simple shear flows of confined rod suspensions, J. Non-Newton. Fluid Mech. 233 (2016) 61–74.
[2] S. Advani, Flow and Rheology in Polymer Composites Manufacturing, Elsevier, 1994.
[3] G.B. Jeffery, The motion of ellipsoidal particles immersed in a viscous fluid, Proc. R. Soc. Lond. Ser. A 102 (1922) 161–179.
[4] C. Petrie, The rheology of fibre suspensions, J. Non-Newton. Fluid Mech. 87 (1999) 369–402.
[5] C. Binetruy, F. Chinesta, R. Keunings, Flows in Polymers, Reinforced Polymers and Composites. A Multiscale Approach, Springerbriefs, Springer, 2015.
[6] G. Taylor, The motion of ellipsoidal particles in a viscous fluid, Proc. R. Soc. Lond. Ser. A 103 (1923) 58–61.
[7] B.J. Trevelyan, S.G. Mason, Particle motions in sheared suspensions I. Rotations, J. Colloid Sci. 6 (1951) 354–367.
[8] F.P. Bretherton, The motion of rigid particles in a shear flow at low Reynolds number, J. Fluid Mech. 14 (2) (1962) 284–304.
[9] E.J. Hinch, L.G. Leal, The effect of Brownian motion on the rheological properties of a suspension of non-spherical particles, J. Fluid Mech. 52 (1972) 683–712.
[10] E.J. Hinch, L.G. Leal, Constitutive equations in suspension mechanics. Part I, J. Fluid Mech. 71 (1975) 481–495.
[11] E.J. Hinch, L.G. Leal, Constitutive equations in suspension mechanics. Part II, J. Fluid Mech. 76 (1976) 187–208.
[12] E.J. Hinch, L.G. Leal, Rotation of small non-axisymmetric particles in a simple shear flow, J. Fluid Mech. 92 (1979) 591–607.
[13] K. Moses, S. Advani, A. Reinhardt, Investigation of the fiber motion of fiber motion near solid boundaries in simple shear flow, Rheol. Acta 40 (2001) 296–306.
[14] C.A. Stover, C. Cohen, The motion of rodlike particles in the pressure-driven flow between two flat plates, Rheol. Acta 29 (1990) 192–203.
[15] C. Jayageeth, V.I. Sharma, A. Singh, Dynamics of short fiber suspensions in bounded shear flow, Int. J. Multiph. Flow 35 (2009) 261–269.
[16] A. Ozolins, U. Strautins, Simple models for wall effect in fiber suspension flows, Math. Model. Anal. 19 (1) (2014) 75–84.
[17] R.B. Bird, C.F. Curtiss, R.C. Armstrong, O. Hassager, Dynamic of Polymeric Liquid, vol. 2: Kinetic Theory, John Wiley and Sons, 1987.
[18] A. Scheuer, E. Abisset-Chavanne, F. Chinesta, R. Keunings, Second-gradient modelling of orientation development and rheology of dilute confined suspensions, J. Non-Newton. Fluid Mech. 237 (2016) 54–64.
[19] P. Brunn, The slow motion of a rigid particle in a second-order fluid, J. Fluid Mech. 82 (1977) 529–547.
[20] L.G. Leal, The slow motion of slender rod-like particles in a second-order fluid, J. Fluid Mech. 69 (1975) 305–337.
[21] H. Giesekus, Die simultane translations-und rotations bewegung einer kugel in einer elastovisken flussigkeit, Rheol. Acta 3 (1963) 59–71.
[22] D. Borzacchiello, E. Abisset-Chavanne, F. Chinesta, R. Keunings, Orientation kinematics of short fibres in a second-order viscoelastic fluid, Rheol. Acta 55 (5) (2016) 397–409.
[23] G. D'Avino, P.L. Maffettone, Particle dynamics in viscoelastic liquids, J. Non-Newton. Fluid Mech. 215 (2015) 80–104.
[24] S. Advani, C. Tucker, The use of tensors to describe and predict fibre orientation in short fibre composites, J. Rheol. 31 (1987) 751–784.